THE USE OF PRINCIPAL COMPONENTS FOR FOR CREATING IMPROVED IMAGERY FOR GEOMETRIC CONTROL POINT SELECTION

MARC L. IMHOFF
NASA/Goddard Space Flight Center
Greenbelt, Maryland 20771, U.S.A.

ABSTRACT

A directed principal component (PC) analysis and its transformation was applied to 7-channel Thematic Mapper Simulator (TMS) data and 4-channel Landsat multispectral scanner system (MSS) data collected over the city of Lancaster, Pennsylvania, to create improved imagery for geometric control point selection for image to image registration.

The analysis was controlled so that the transformation matrix was generated from statistics gathered only on the urban and high density residential areas in order to enhance the infrastructural features desired for geometric control point selection.

Nineteen temporally stable geometric control points, such as road intersections and bridges, were selected for a 236 km^2 area using USGS 7½ minute topographic quadrangles and color infrared photography. The control points were visible on both the TMS and MSS imagery. On the first attempt the corresponding image control points were selected on both data sets without using the principal components transformation. Many of the road intersection locations were visible but the actual road crossings could not be distinguished. As a result, mensuration errors using raw data exceeded the equivalent of two (79 x 79 m) pixels. The application of a guided principal components transformation yielded TMS and MSS single band images showing improved detail in the scene's urban and residential infrastructure. The PC transformed data sets were then utilized for the reselection of geometric control points. By showing greater detail, control points on both the TMS and MSS imagery could be located with greater precision using the PC transformed data. Control point reselection after transformation resulted in a 50 percent decrease in registration error.

1.0 INTRODUCTION

Accurate geometric correction and cartographic registration is an important factor in making use of remotely sensed image data. In an era of increasing interest and development of geographic information systems (GIS) it is imperative that the many data layers included in these systems be geometrically matched or registered to one another. In the case of remotely sensed imagery this becomes particularly important not only for ultimate input to a GIS but also for the creation of merged multisource data sets suitable for spectral and spatial analysis.

Image to image geometric registration can be complicated by a number of basic factors:

1. spatial differences due to differing ground instantaneous fields of view (GIFOV) between data collection instruments,

2. platform differences (satellite vs. non-satellite, etc.),

3. spectral differences (i.e., differing number of bands and band widths.

When dealing with data of two or more differing spatial resolutions, one is confronted with the problem of multiple resampling. A resampling must occur in order to produce the images in a common pixel size and then again to geometrically register the images to a particular geometric base. Even when that process is accomplished in one routine, the data is degraded. Various resampling techniques represent tradeoffs in their effects on image geometry as well as the density numbers (DN) associated with each pixel (T. L. Logan and A. H. Strahler, 1979). Nearest neighbor best preserves original DN values but creates a moiré pattern in the imagery causing registration accuracy to vary considerably throughout the image (Jayroe, 1976). Cubic convolution and bilinear interpolation appear to be the best techniques for resampling imagery for input to a GIS; however, in both cases the original (DN) values of the data are altered. A comprehensive review of interpolation techniques, complete with an excellent list of references can be found in a work by Billingsley (1982).

Another problem caused by differing spatial resolutions between imagery is areal measurement. Even after resampling an image the basic areal extent of a particular target feature will remain the same as it was before resampling. A river system or roadway, for example, imaged by two instruments with different IFOV's will record two different areal measurements associated with those same features. This becomes a particularly annoying problem when one overlays imagery containing such features as winding rivers and/or roadways where not only do their widths vary but the concave-convex curve areas for those targets differ appreciably as well.

Platform differences can also cause complications. Imagery collected from an airborne instrument platform will have a number of geometric and radiometric distortions due to sun angle, aircraft pitch, yaw, roll, aircraft and instrument jitter, etc., that are only minimally present in satellite data. Unfortunately, these effects are of fairly high spatial frequency and difficult to model and remove.

Spectral differences complicate matters by splitting the scene into a number of separate bands or images. The advantage of splitting an image up into spectral bands for spectral modeling often complicates ground control point selection. In an infrastructural setting, for example, some road systems, depending upon the reflectance characteristics of the surface material, appear well only on a particular band width. It is often necessary to look at all the bands in a data set to

build a complete picture of a road network. Obviously, in dealing with two sets of multiband data different in their band widths and number of bands, the matter of matching the road networks becomes even more complicated.

While spatial differences and platform differences between data inputs present more complex registration problems, the spectral problem of multiband image handling can be more easily solved.

2.0 PURPOSE

The objective of this study was to develop a simple technique designed to improve the accuracy of ground control point selection for geometric correction and registration of multiband and multisource imagery. The transformation used was selected such that it was currently available and a relatively standard accessory to most digital image processing packages. This was done in order that the technique presented here be immediately implementable by a majority of the user community.

Principal components analysis and its transformation was selected due to its relative simplicity and general availability. Jet Propulsion Laboratory's VICAR, ESL's IDIMS, and the Pennsylvania State University's ORSER system all have principal components options. Principal components is a technique whereby a new set of axes is defined for the data such that the first principal component or axis explains as much of the total variance as can be explained by any single variable or axis. The second principal component or axis explains as much of the remaining variance as can be explained by any axis orthogonal (uncorrelated) to the first. The third principal component continues this process and so on until the dimensionality of the data is exhausted (Merembeck and Borden, 1978). The effect is that most of the information inherent in the many spectral bands is combined or explained by one, two, or three of the principal components. The technique was used here to create improved single band imagery for geometric control point selection. In this example, the control points were used for image to image registration of two different types of remotely sensed data, airborne Thematic Mapper Simulator (TMS) and satellite Landsat Multispectral Scanner System (MSS) data. In this case a directed principal components analysis was used to focus the transformation around such infrastructural features as road networks, housing developments, and urban areas.

3.0 MATERIALS AND METHODS

The two images used in this study were a 7-channel TMS data set and a 4-channel Landsat MSS data set. Both sets of image data were collected over the city of Lancaster, Pennsylvania (Figure 1).

The TMS data is composed of 7 bands (0.45-0.52, 0.52-0.60, 0.63-0.69, 0.76-0.90, 1.55-1.75, 2.08-2.35, 10.4-12.5 μm), has a GIFOV of 30 x 30m and was collected from an airborne Learjet aircraft (ORI, 1982).

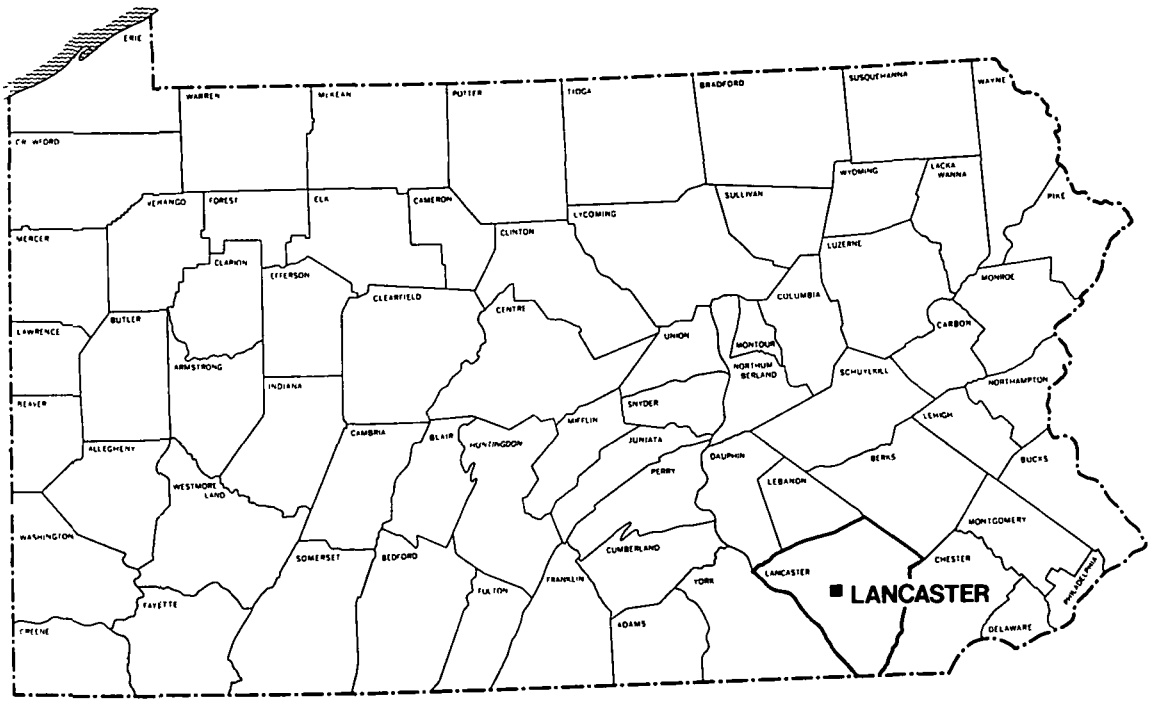

Figure 1: Study site, the city of Lancaster Pennsylvania

The TMS data suffered from several problems:

1. Considerable image distortions due to aircraft roll, pitch, and yaw were apparent in all bands.

2. A high frequency spatial distortion possibly due to aircraft and/or instrument jitter was also present in all bands.

3. Calibration problems and electronic noise also appeared in the imagery in the form of line striping and beat patterns.

The satellite data was Landsat-2 data tape ID# 21660-15011. It consisted of 4 spectral bands (0.5-0.6, 0.6-0.7, 0.7-0.8, 0.8-1.1 μm) and was resampled to create a 79 x 79 meter pixel. Some slight line striping was present in bands 1 and 2; however, for the most part the data quality was quite good.

The survey site consisted of a 236 km^2 area centered over the city of Lancaster, Pennsylvania. The equipment used to display, locate, transform, and analyze the image data consisted of a DeAnza image display system interfaced with ESL's IDIMS software implemented on an HP 3000 computer.

Ground control points were selected from USGS 7½ minute topographic quadrangles and color infrared photography. Nineteen widely scattered points were selected. The ground control points consisted of road intersections, street corners, and bridges. The ground control points selected were relatively stable over time and generally visible in all seasons of the year. Although the ground control points were visible on both data sets, it was necessary to view all of the MSS bands and four of the TMS bands (2, 4, 6, and 7) to accurately locate the exact position of the control points. This problem was found to be most prominent where highways composed of varying surface materials intersected or where a bridge passed over water.

Using the raw data sets the ground control points were located and their image coordinates fed into separate image mensuration files. Precise location of the control points using the raw data sets proved difficult. Many of the road intersections were visible but the actual road crossings could not be distinguished even using the three color (band) composite capability of the DeAnza image display.

When all 19 points were located as carefully as possible, the corresponding sets of mensuration data were input to an algorithm where a transformation matrix was generated using a least-squares fit method. The transformation was then applied to the TMS mensuration file and the resultant points were subtracted from the MSS mensuration file in order to determine residuals. All transformations for this study were carried out only to the first order for simplicity. The list of source (TMS) and destination (MSS) control points and their residuals for the raw data sets (Table 1) reveal errors in excess of 2.6 pixels in the x direction and 1.6 pixels in the y direction (residuals are measured in terms of Landsat 79 x 79m pixels).

In an effort to improve the accuracy of control point location, a directed principal component analysis was performed on the TMS and MSS imagery. A directed principal components transformation differs from general principal components in that instead of using statistics describing the general shape of the whole data swarm in four dimensional space, the statistics are derived from a subset of the data describing the target surface feature or features.

A simple polygon targeting training site selection and statistical calculation program was used to derive means and variance-covariance statistics for a specified region of the imagery. A polygon was defined that delineated only the more heavily urbanized areas supporting a large proportion of region's infrastructure. Only the urban areas, highway strip developments and high density residential areas were utilized for statistics definition. A set of correlation matrices were generated comparing the raw and transformed data sets for both the MSS and TMS data (figures 2 and 3).

MSS axes 1 and 2 had high correlations with MSS raw bands 1 and 2 (.5-.6 μm and .6-.7 μm). This is not surprising since those bandwidths best describe rock, soil and manmade features. The relationship between the TMS transformed data (axes) and the TMS raw data is a little more complicated. With the exception of band 7 (thermal), no single raw band has appeared to contribute an inordinately large proportion of information to the principal components. Instead the principal components seem to be "extracting" nearly equal amounts of information from each of the raw bands.

The transformation based on the statistics for these areas reduced the data dimensionality and yielded imagery showing improved detail in the scene's urban and residential infrastructure (figures 4 and 5). TMS axis 1 portrayed roadways, intersections, and residential housing plans much more clearly than any other single band or 3-channel combination of the raw data.

The Landsat MSS data was also improved by the transformation. MSS axes 1 and 2 showed as much infrastructural detail as all four of the raw bands. The transformed data was used for the reselection of the previously defined ground control points.

The new control point coordinates for the TMS and MSS data were entered into mensuration files and the least-square fit method of determining the transformation matrix and residuals was repeated.

4.0 RESULTS AND CONCLUSIONS

The geometric registration of remotely sensed data sets is an important factor in creating useful multisource composite imagery and input imagery for geographic information systems. Any improvement in geometric control point selection speed and accuracy is of great value to the process of GIS data entry.

FIGURE 2: CORRELATION MATRIX FOR MSS DATA
PC AXES VS. UNALTERED BANDS

UNALTERED BANDS	PC Axes 1	2	3	4
1	.96	.31	-.01	.20
2	.98	.31	.01	-.16
3	.36	.96	.20	.01
4	-.17	.92	-.20	-.03

* correlations are for urban targets only

FIGURE 3: CORRELATION MATRIX FOR TMS DATA
PC AXES VS. UNALTERED BANDS

UNALTERED BANDS	PC Axes 1	2	3	4	5	6	7
1	-.38	.60	-.63	.13	-.05	.34	-.21
2	-.50	.68	-.58	.21	.02	-.06	.07
3	-.47	.68	-.63	.27	.06	-.15	-.13
4	-.62	.24	.54	.03	.13	-.02	.03
5	-.62	.54	-.02	.61	-.11	-.04	-.01
6	-.42	.57	-.32	.51	.57	.01	-.05
7	.85	.64	-.07	-.02	.01	-.02	.01

* correlations are for urban targets only

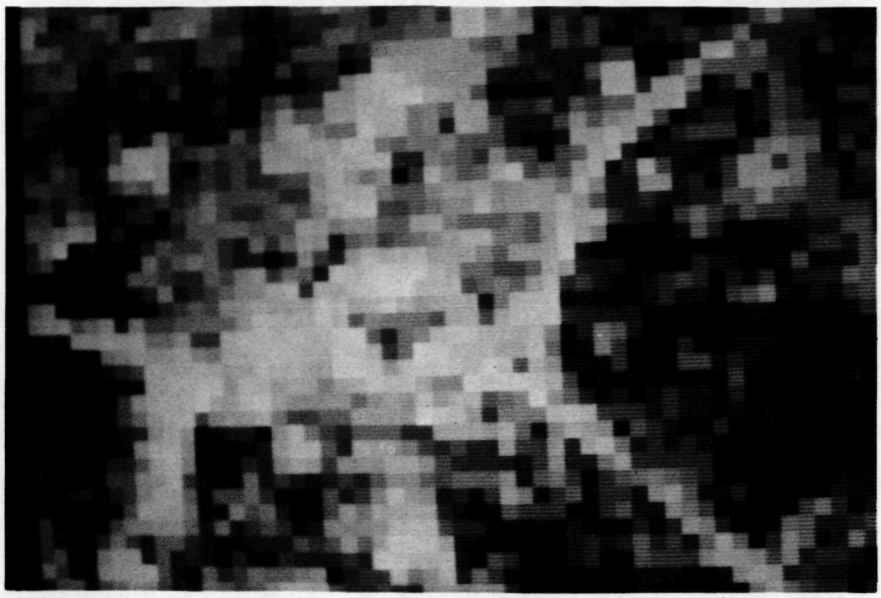

Raw MSS band 6

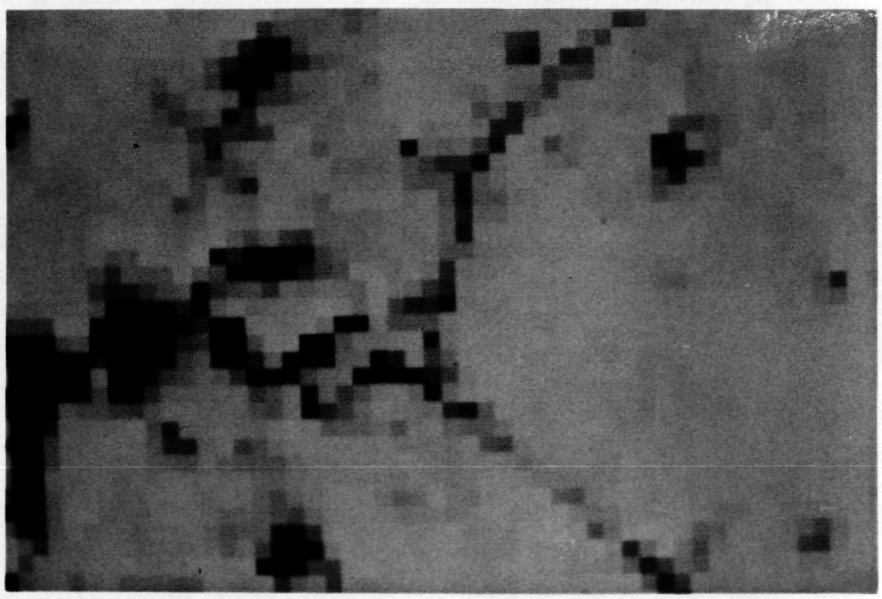

MSS principal component axis 1

FIGURE 4: Raw MSS imagery and MSS principal component axes 1 image depicting a road intersection

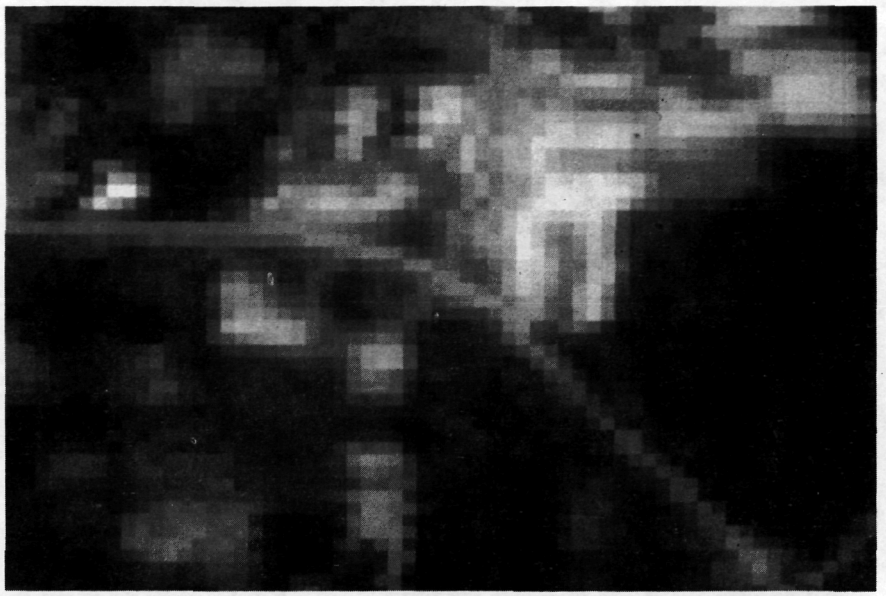

TM simulator band 4

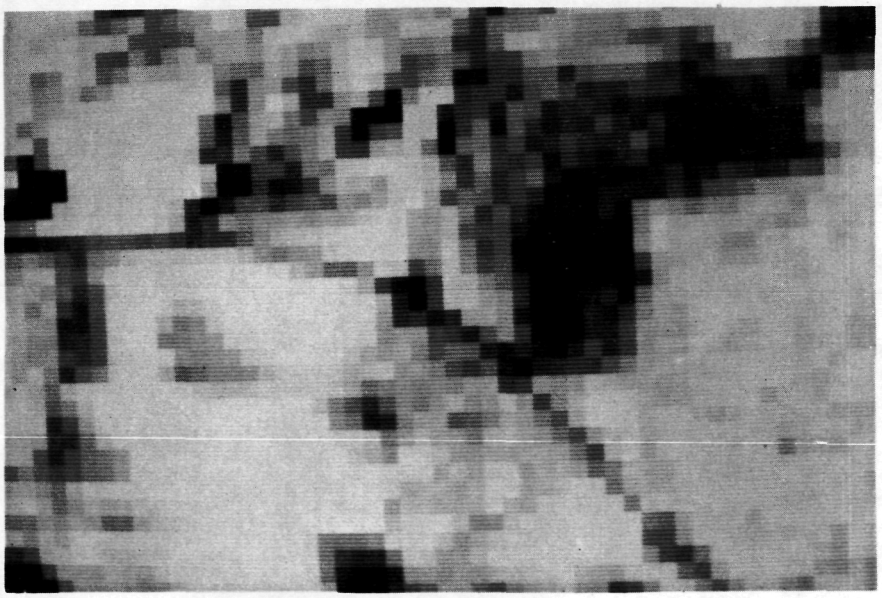

TM simulator principal component axis 1

FIGURE 5: Raw TM simulator imagery and TM simulator principal component axis 1 depicting a road intersection

By showing greater detail of the infrastructural features, the principal components transformed image data allowed for a more accurate delineation of the ground control point locations. Road intersections could be more precisely located eliminating errors in their coordinate definition. The residuals from the least squares derived geometric transformation revealed that the control point reselection using the principal components enhanced data resulted in a combined 52 percent decrease in registration error. The x and y simple means of the residuals were reduced from 2.67 and 1.63 pixels for the raw data to 1.14 and 0.86 pixels for the principal components data (Tables 1 and 2). This represented a 57 percent reduction in error in x direction and a 47 percent reduction in locational error in the y direction.

In conclusion, a directed principal components analysis and its transformation can provide a valuable means for improving registration accuracy between remotely sensed imagery.

The technique provided single band imagery with improved target feature definition. The use of single band imagery expedited the ground control point selection process as it required less time to access, display and expand the single band imagery. The use of a single band display also eliminated potential resolution problems caused by color gun alignment within the display device. The technique is straightforward, consumes little time (30 minutes for complete analysis and transformation of a 1000 x 500 7-channel data set), and in this case provided a significant increase in accuracy.

TABLE 1: List of source, destination, and transformed coordinates and the residuals for control point matching using raw MSS and TMS data

GROUND CONTROL POINT		SOURCE (TMS)		DESTINATION (MSS)		TRANSFORMED		RESIDUALS	
		SX	SY	DX	DY	TX	TY	RX	RY
1	AX	194	474	217	213	216	212	1.4	.9
2	AR	77	670	176	288	165	296	10.7	-8.4
3	AM	224	706	230	314	235	313	-5.1	1.5
4	AN	139	550	191	245	192	245	-.6	.2
5	AD	94	459	171	208	168	205	2.6	2.7
6	AH	313	367	269	164	269	166	-.0	-2.3
7	AO	192	582	217	260	217	259	-.2	1.2
8	AI	255	520	246	233	245	232	.7	.7
9	AJ	249	613	242	275	245	272	-2.7	2.6
10	AK	263	586	249	262	251	261	-1.6	1.2
11	AL	324	550	280	246	278	245	1.6	.5
12	AG	328	478	281	214	279	214	2.4	-.4
13	AC	151	449	195	203	195	201	.1	1.8
14	AE	191	420	209	188	213	189	-4.0	-.8
15	AB	240	432	238	195	236	194	1.7	.8
16	A1	292	441	262	198	261	198	1.1	-.3
17	AQ	177	691	209	306	213	306	-3.7	.1
18	AF	377	320	301	143	298	146	3.0	-3.3
19	AS	126	379	174	172	182	171	-7.6	1.2
RESIDUAL MEANS		=	2.67	1.63					

TABLE 2: List of source, destination, and transformed coordinates and the residuals for control point matching using single band PC transformed MSS and TMS data

GROUND CONTROL POINT		SOURCE (TMS)		DESTINATION (MSS)		TRANSFORMED		RESIDUALS	
		SX	SY	DX	DY	TX	TY	RX	RY
1	AR	99	665	171	295	172	297	-1.1	-1.7
2	AM	226	706	230	314	232	314	-2.4	.3
3	AS	126	379	181	173	183	172	-2.2	1.0
4	AF	377	320	301	143	302	145	-.6	-1.6
5	AQ	177	691	209	306	209	308	-.2	-1.5
6	A1	292	441	262	198	262	198	-.1	.1
7	AB	240	432	238	195	237	194	.6	.7
8	AE	191	420	214	189	214	189	-.2	-.4
9	AC	151	449	195	203	195	202	-.4	.7
10	AG	328	478	281	214	279	214	1.6	.3
11	AL	324	550	280	246	278	245	2.1	.9
12	AK	263	586	249	262	249	261	-.2	.8
13	AJ	249	613	242	275	243	273	-.8	1.9
14	AI	255	520	246	233	245	233	.9	.5
15	AO	192	582	217	260	216	260	1.4	.0
16	AH	313	367	269	164	272	165	-2.6	-1.5
17	AD	94	459	171	208	169	207	2.5	.9
18	AN	139	550	191	245	190	246	.6	-1.4
19	AX	194	474	217	213	216	213	1.1	.1

RESIDUAL MEANS = 1.14 .856

BIBLIOGRAPHY

Billingsley, F. C., 1982. Revised Edition of The Manual of Remote Sensing, Chapter 17, American Society of Photogrammetry.

Jayroe, R. R., Jr., 1976. Nearest Neighbor, Bilinear Interpolation and Bicubic Interpolation-Geographic Correction Effects on Landsat Imagery, NASA Technical Memorandum TMX-73345, Marshall Space Flight Center.

Logan, T. L., and A. H. Strahler, 1979. The Errors Associated with Digital Resampling of Landsat Forest Imagery for Multidate Registration, Eighth Annual Remote Sensing of Earth Resources Conference, The University of Tennessee Space Institute, Tullahoma, Tennessee.

Merembeck, B. F., and F. Y. Borden, 1978. Principal Components and Canonical Analysis for Reduction of the Dimensionality of Large Data Sets. Technical Report 5-78, Office for Remote Sensing of Earth Resources, The Pennsylvania State University, University Park, Pennsylvania.

ORI. Renewable Resources Thematic Mapper Simulator Workshop, Technical Report 1907k ORI, Silver Spring, Maryland.